KSCE Journal of Civil Engineering (2018) 22(2):637-646

DOI 10.1007/s12205-017-1089-5

Structural Engineering

pISSN 1226-7988, eISSN 1976-3808
www.springer.com/12205

Effects of Crack Width on Chloride Penetration and Performance Deterioration of RC Columns with Sustained Eccentric Compressive Load

Papa Niane Faye*, Yinghua Ye, and Bo Diao*****

Received December 26, 2015/Revised August 11, 2016/Accepted March 9, 2017/Published Online May 22, 2017

Abstract

In a marine environment, the mechanical performance of Reinforced Concrete (RC) structures deteriorates mainly due to the coupling action of service load and/or the corrosion of steel bars. Here, the working conditions of RC columns in a marine environment were simulated in the laboratory. The chloride penetration and performance deterioration of RC columns with different widths for the maximum initial crack of 0, 50, 100 and 200 microns, induced by different levels of external sustained eccentric compressive load and environments of chloride corrosion, were simulated by seawater wet-dry cycles. The results showed that the yielding load and ultimate load of the RC column specimens were significantly decreased as the width of the initial cracks increased. Tensile strain and crack width were both parameters contributing to chloride penetration in the tensile area of the RC column specimens. During the seawater wet-dry cycles, the initial cracks on the column specimens changed. The initial cracks tended to vanish due to the self-healing capacity of concrete when the width of the initial crack was smaller than 50 microns. The initial cracks remained relatively constant when the crack widths were between 50 and 100 microns, and the crack widths increased when the initial crack width was larger than 100 microns.

Keywords: *crack width, tensile strain, sustained load, reinforced concrete column, wet-dry cycle, chloride penetration*

1. Introduction

The durability of a Reinforced Concrete (RC) structure is the ability of the structure to maintain its safety and suitability during its service life. The research progress of concrete structural durability can be divided into the materials of the concrete or steel bars, reinforced concrete members or structures of two levels in different environments. The environment of the exposed concrete structure can be classified as an ordinary atmospheric environment, a marine environment, an industrial environment, etc.

At the material level, many experiments with concrete material have been performed to investigate the durability in different environments. It was concluded (Gu *et al*., 2015) that the crack geometry is the key factor that influences the chloride transport process in the crack, and the cracked concrete information should include the width, depth, tortuosity, connectivity and surface roughness of the crack. The penetration and the content of chloride depend on the porosity and the permeability of the concrete cover (Lu *et al.*, 2011), the age of the concrete and the stress states (Malumbela *et al.*, 2009). Cracks in concrete may act as flow channels for an aggressive medium such as chlorides, accelerating the rate of chloride ingress and, hence, the onset of corrosion (Djerbiet *et al*., 2008). The investigations "Comparison of Chloride Ion Penetration and Diffusion of High-Performance Concrete" (Khan, 2012) and "Examination on Chloride Penetration through Micro-Crack in Concrete" (Yoon *et al*., 2014) affirmed that chloride content decreased with an increase in the depth of penetration. Current codes disregard the influence of loading cracks of reinforced concrete members when the width is smaller than 100 microns in a marine environment (Jia *et al*., 2010). The permeability increases rapidly when the crack width increases from 50 microns to approximately 200 microns. After the crack width reaches 200 microns, the permeability increases steadily (Ismail *et al.*, 2008; Marsavina *et al*., 2009). Visual inspection shows that, almost always, corrosion started at cracked sections for all tested beams (LI, 2001). When reinforcement corrosion develops, the corrosion products accumulating at the rebar surface are expansive, and their volume depends on the type of oxide and the degree of hydration (Khan *et al*., 2014). Therefore, concrete structures in coastal regions could deteriorate due to damage from both chloride corrosion and concrete cracks during

*Ph.D. Student, Dept. of Civil Engineering, BeiHang University, Beijing 100191, China (Corresponding Author, E-mail: papanf@buaa.edu.cn)
**Professor, Dept. of Civil Engineering, BeiHang University, Beijing 100191, China; State Key Laboratory of Subtropical Building Science, South China University of Technology, Guangzhou 510641, China (E-mail: yhye@buaa.edu.cn)
***Professor, Dept. of Civil Engineering, BeiHang University, Beijing 100191, China; State Key Laboratory of Subtropical Building Science, South China University of Technology, Guangzhou 510641, China (E-mail: diaobo@buaa.edu.cn)

their service lives.

On the level of RC members or structures, performance deterioration is caused mainly by the corrosion (acids and/or salts) of steel bars and by physical damage (external loads or freeze-thaw cycles). The corrosion of steel bars in concrete structures is the predominant factor in the premature deterioration mechanisms (Li, 2001; Zhao *et al*., 2011), leading to the loss of the bond between the steel and the concrete and the loss of the area of the steel bars (Malumbela *et al*., 2009), as well as the loss of bearing capacity and ductility of the structures (Capozucca *et al.*, 2000). During the life time of RC structures, some microcracks or capillaries in concrete may be partially closed by compressive stresses (Gowripalan *et al*., 2000) or create tensile cracks in the concrete when the tensile stress is larger than the tensile strength (Malumbela *et al.*, 2009).The initial crack width is directly proportional to the reinforcement strain (Noël *et al*., 2014). Specifications of RC structure have been clearly defined to provide the functions of safety, stability and durability. When the durability of the concrete structure is damaged, first, the physical, chemical and geometric shapes of the concrete or steel bar material change. Second, the damage to the durability of the structure causes the decay of the bearing capacity and will finally affect the safety of the entire structure (Pachecoetal, 2014). Field engineers estimating the condition of cracked structures are basically limited to crack width measurements at the concrete surface. Today, the relationship between the crack width and the durability performance in a chloride environment remains unclear. However, crack width and cover thickness become the most practical parameters for the durability assessment of RC structures (Lu *et al.*, 2011).

The multiple damage effects of chloride corrosion and widening of loading cracks on the degradation of RC structures remain a challenge for civil engineers. Many studies have been done to understand the behavior of structures in a coastal environment, and several materials have been used to enhance the performance of concrete in a marine environment. Therefore, it is necessary to investigate the effects of crack widths on the deterioration of RC members under wet-dry cycles in seawater. Here, the working conditions of the RC structures were simulated in the laboratory to understand the effects of the loading crack on the performance deterioration of RC members in a chloride environment, as well as the effects of crack width on the chloride penetration of RC members.

2. Specimens and Test Program

2.1 Concrete Mixture and Design of Specimens

The effects of the initial crack width due to sustained eccentric compressive load on the chloride penetrability and the structural deterioration of the RC column specimens were investigated experimentally. A total of five RC column specimens and five groups of plain concrete prism specimens were cast. The proportions of the concrete mixture are listed in Table 1, and the testing conditions for the RC column specimen are described in Table 2.

The air content of the concrete was measured using the pressure method of the American Society for Testing and Materials ASTM C231 (2010). The air content of the concrete mixture was 5.7%, with a maximum aggregate diameter of 10 mm. The compressive strength of the concrete prism with a size of 100 mm × 100 mm × 300 mm was 39.3 MPa, tested at the age of 28 days.

The reinforced concrete column specimens were designed with a rectangular cross-section in the middle-height segment, which was reinforced with four longitudinal steel bars with 10 mm diameters, with stirrups of 6 mm diameter and a concrete

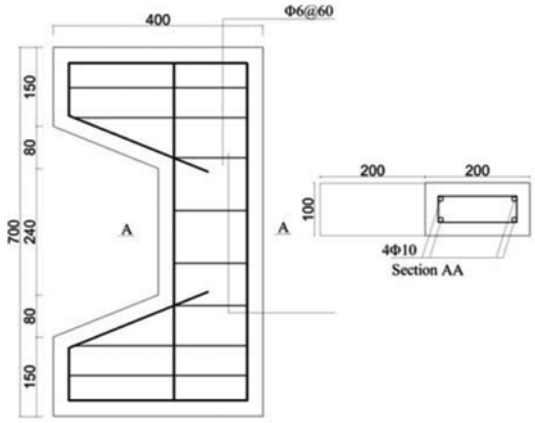

Fig. 1. Geometry and Rebar Arrangement of RC Column Specimens

Table 1. Concrete Mixture kg/m^3

Designation	Water	Cement	Fly ash	Sand	Aggregate	Water Reducer	Air Entertainer
Quantity	184	460	53	609	1130	3.94	100.61

Table 2. Testing Condition of Five Column Specimens

RC Column Specimen	Sustained Load Values (kN)	Stresses of Tensile Steel Bar (MPa)	Max. Width of Initial Crack W_d (microns)	Exposed Environment	Test Age of Static Loading
Z1	none	None	0	atmosphere	128d
Z2	none	None	0	Wet-dry	128d
Z3	26	30.56	50	Wet-dry	128d
Z4	33	46.80	100	Wet-dry	128d
Z5	67	148.34	200	Wet-dry	128d

cover to a reinforcement of 30 mm. Two brackets were designed at both ends of the column specimen to apply a sustained eccentric compressive load. The geometric sizes and arrangement of steel bars of all five RC column specimens were the same and are shown in Fig. 1.

2.2 Test Program

A total of five RC column specimens were cast and cured under laboratory conditions for 28 days and then exposed to two environments in the structural laboratory of BeiHang University. As listed in Table 2, column specimen Z1 was exposed to an atmospheric environment (natural laboratory environment), as a reference specimen. Four other column specimens Z2~Z5 were produced with different widths for the initial cracks using different levels of sustained eccentric compressive loading and then were exposed to wet-dry cycles of seawater. The wet-dry cycles of seawater included 8 hours of immersion in seawater and 16 hours of exposure in the atmospheric environment, where the seawater was artificially made at a concentration of 3%NaCl+0.34%Na_2SO_4.

A total of four groups of plain concrete specimens were cast and accompanied by the five PC column specimens. At the age of 28 days, one group (3 specimens) was tested to determine the concrete compressive strength. Then, three out of four remaining groups of three concrete prism specimens each were exposed to 25, 50 and 75 cycles of seawater wet-dry, respectively, and then the compressive strengths were tested.

At the age of 28days, the eccentric compressive load was applied to column specimens Z2, Z3, Z4 and Z5 to produce the maximum widths of an initial crack of 0, 50, 100 and 200 microns, respectively. As shown in Fig. 2(a) and the photo in Fig. 2(b), the eccentric compressive load was applied by tightening the blind nut, and the load was sustained until the design cycles of seawater wet-dry were finished. Here, the number of the design cycles was 90. The eccentric sustained load values of the RC column specimens and the corresponding stresses of tensile

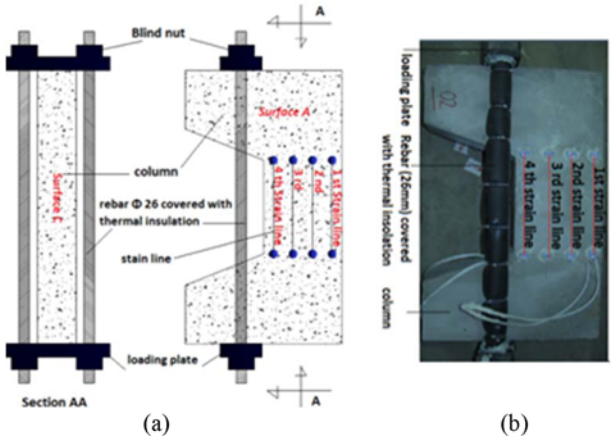

Fig. 2. Application of Eccentric Sustained Load on the Column and Thermal Insulation Protection: (a) Application of Eccentric Load on the Column, (b) Thermal Insulation of Loading Bar

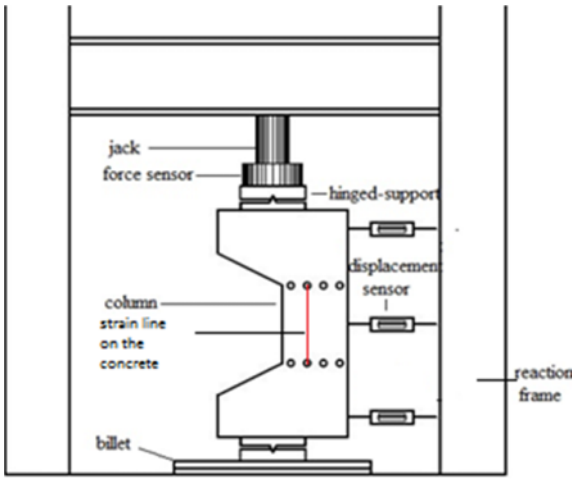

Fig. 3. Static Loading Experiments

steel bars are listed in Table 2, where the stresses of tensile steel bars were calculated by the measured strain.

During the wet-dry cycles, after each 15 cycles of wet-dry, i.e., 15, 30, 45, 60, 75, 90 cycles, the crack widths the longitudinal strains of the concrete were measured on the concrete surface at the middle segment of each column specimen along four strain lines, as shown in Fig. 2(a). At the age of 118 days (after 90 cycles of wet-dry), the last strain values and crack widths were measured before and after the sustained load was removed.

After the sustained load was removed, all five RC column specimens were static-loaded to test their remaining bearing capacities, where the transversal displacement of columns and tensile strain of steel bars were tested and collected on a computer, as shown in Fig. 3.

After static loading was completed, the chloride content of the concrete was tested in the tensile area along the axial length of the RC column specimens. Cylinder samples of concrete with 50 mm diameters and 30 mm depths were drilled from the tensile area (Surface C) of the RC column, and then the samples were divided along the depth into 3 round sheets of 10 mm each. The concrete round sheets were ground to powder to test the chloride content of the specimens. The chloride content of concrete was tested in the tensile area, which was divided into the cracked and un-cracked areas of the cracked columns (Z3, Z4 and Z5).

3. Test Result Analysis Anddiscussion

During the experimental process, the combined effects of several parameters, such as sustained load, initial crack and chloride corrosion, were investigated by crack development, strain variation, remaining bearing capacity and chloride content. In this part of the paper, the testing results were first analyzed, and then a discussion was conducted to get a clearer view of the interdependency of the parameters studied.

3.1 Test Result Analysis

The details such as crack distribution and evaluation, concrete

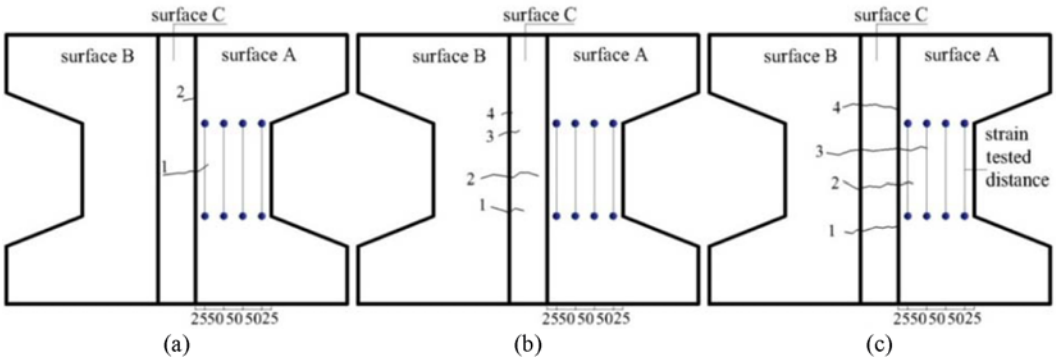

Fig. 4. Distribution of Initial Cracks on RC Column Specimens: (a) Cracks in Specimen Z3, (b) Cracks in Specimen Z4, (c) Cracks in Specimen Z5

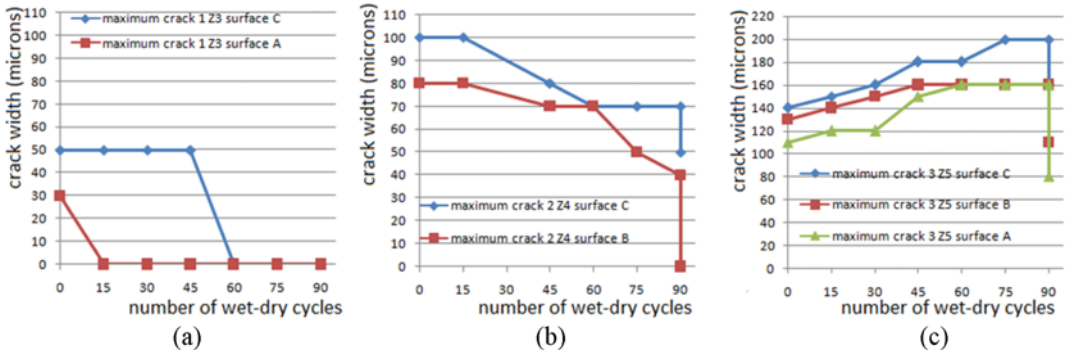

Fig. 5. Crack Evolution on Columns Z3, Z4 and Z5: (a) Crack Evolution on Column Z3, (b) Crack Evolution on Column Z4, (c) Crack Evolution on Column Z5

strain on the middle segment of RC column specimen, remaining bearing capacity and chloride content observed or tested in this experiment were shown and analyzed here.

3.1.1 Crack Cartography and Evaluation

At the age of 28 days, the RC column specimens were progressively eccentrically loaded until the maximum width of the initial crack reached approximately 50 microns, 100 microns and 200 microns on Z3, Z4 and Z5, respectively. The initial crack distributions on the column specimens are shown in Fig. 4 (a, b and c).The RC column specimen was expanded with three surfaces according to tensile crack position, where the three surfaces of the column specimen were called surface A, surface B and surface C.

As shown in Fig. 5(c), the evolution of crack number 3 in specimen Z5 for different cycles of wet-dry was listed in Table 3, where eight testing points were selected.

The evolution of the maximum widths of cracks on RC column specimens Z3, Z4 and Z5 are plotted in Fig. 5. As shown in detail, at the age of 28d (0 cycle), maximum initial crack widths of 0, 50, 100 and 200 microns on the different column specimens were induced by different levels of sustained load, and the crack width changed as the number of wet-dry cycles increased. Fig. 5(a), Fig. 5(b) and Fig. 5(c) show the evolution of

Table 3. Evolution of Crack Width at Crack 3 of Column Specimen Z5 (200 microns)

Cycles and Crack Testing Point N	0 Cycle After Loaded	15 Cycles	30 Cycles	45 Cycles	60 Cycles	75 Cycles	90 Cycles	90 Cycles Load Removed
	Evolution of crack width (microns)							
1	110	120	110	130	130	130	130	110
2	130	130	150	150	150	150	150	110
3	130	130	140	150	150	150	150	110
4	130	130	130	130	150	150	150	100
5	140	150	160	180	180	200	200	160
6	110	120	120	130	130	130	130	100
7	110	110	110	110	110	120	120	70
8	100	100	100	100	100	110	110	70
Maximum crack	140	150	160	180	180	200	200	160

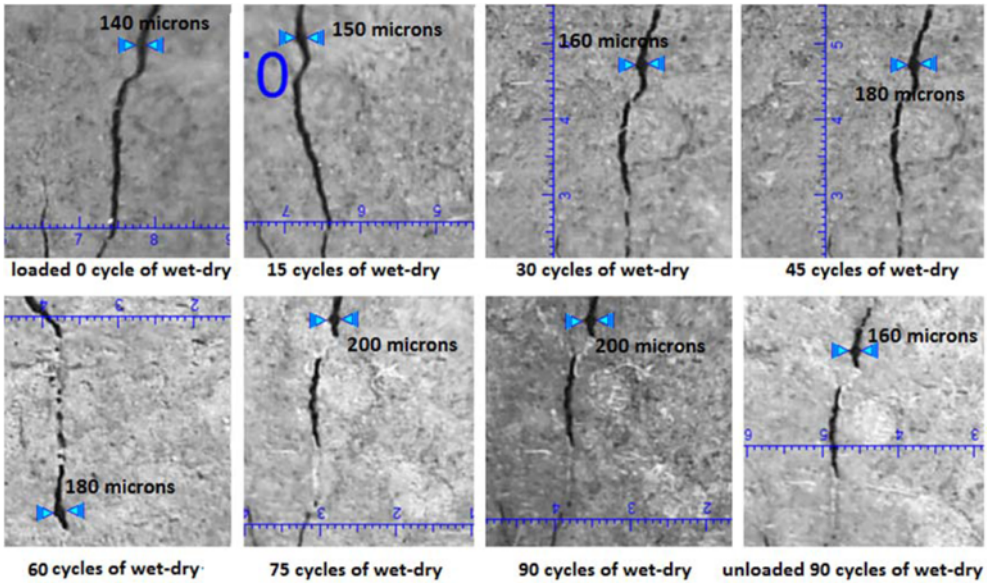

Fig. 6. Evolution of Crack Widths on Column Z5 at Testing Point 5 in Table 3

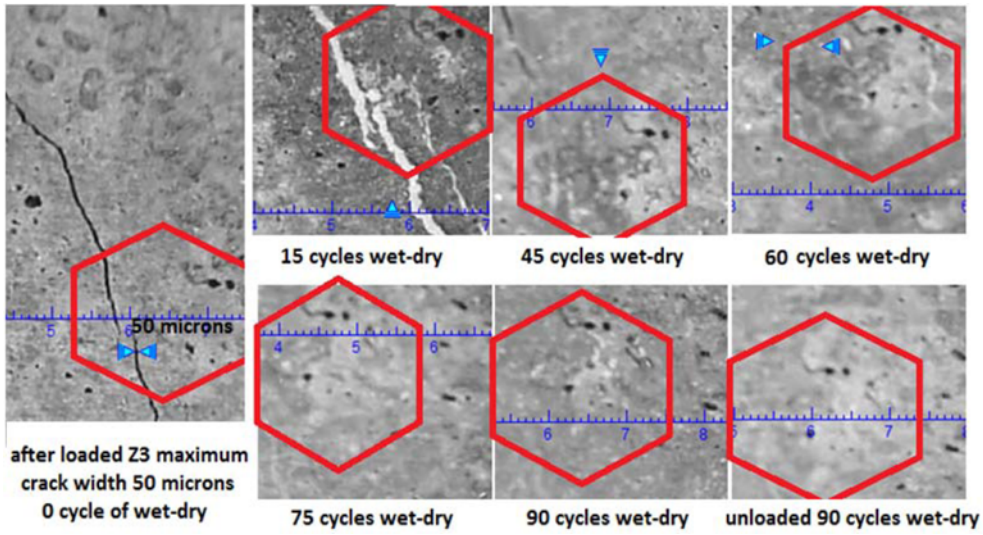

Fig. 7. Width Evolution of Crack 1on Column Z3 with Maximum Width 50 Microns at Surface C

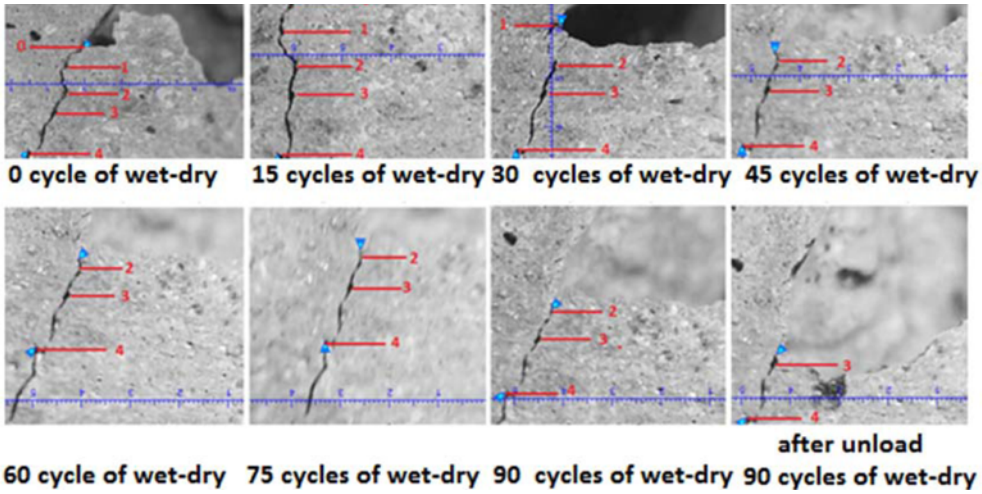

Fig. 8. Photos of Evaluation of the Apparent Concrete Degradation as the Number of Wet-dry Cycles Increase

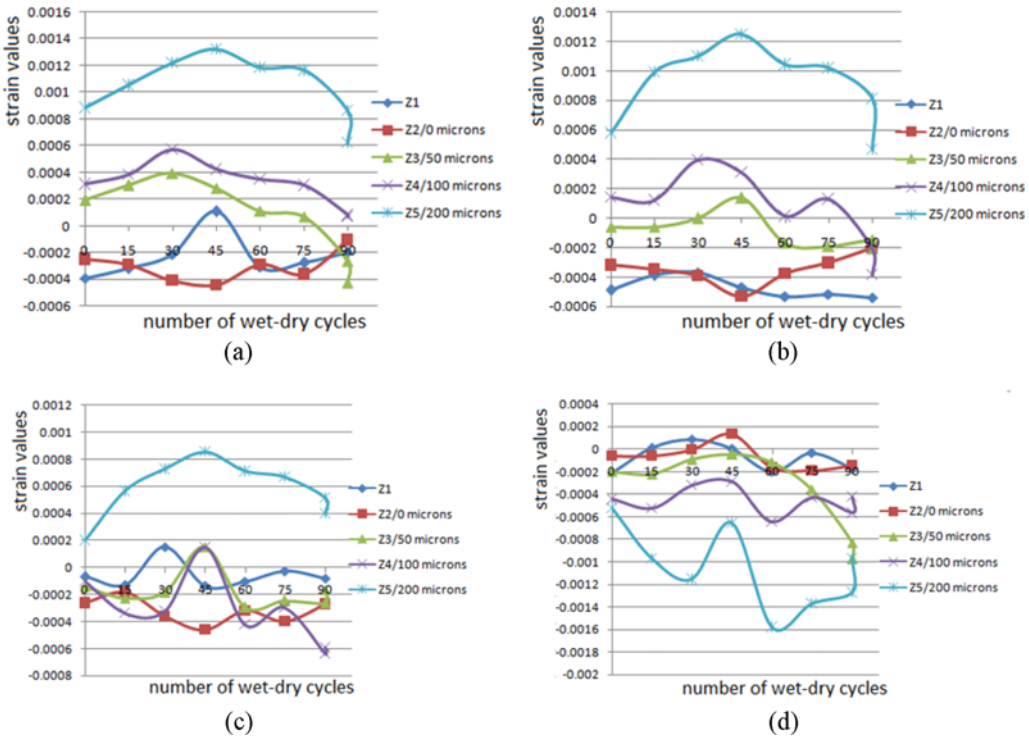

Fig. 9. Strain Evaluation of Column Specimens Under Action of Sustained Load and Wet-dry Cycles: (a) Strain Values for the 1st Strain Line (Fig. 2), (b) Strain Values for the 2nd Strain Line (Fig. 2), (c) Strain Values at for the 3rd Strain Line (Fig. 2), (d) Strain Values for the 4th Strain Line (Fig. 2)

the initial cracks, where all crack widths of column Z3 decreased and became 0 microns after 60 days of wet-dry cycles, the maximum crack width of column Z4 decreased and the maximum crack width of column Z5 increased as the number of wet-dry cycles increased.

The photos in Fig. 6 show the evolution of testing point 5 for crack 3 in column Z5, also listed in Table 3. Fig. 7 shows the evolution of crack 1 (50 microns) on surface C of column Z3.

Around cracks, a degradation of the concrete was observed, as shown in Fig. 8. To understand the degradation of the concrete and give a general view of the crack, five testing points were fixed from the loading time until the end of the wet-dry cycles, as shown in Fig. 8. The testing point 0 was fixed on the column and located at a hole, and the distance between testing point 0 and point 1 was 3.21 mm. After 30 wet-dry cycles, point 1 had already become the boundary of the hole, and the hole arrived at point 2 after 45 wet-dry cycles. Here, based on the origin given by point 0, the hole became larger, which is very detrimental for a reinforced concrete structure in a marine environment.

3.1.2 Strain Testing on Surface Concrete

During the period of wet-dry cycles, longitudinal concrete strains on the middle segment of the column specimen, as shown in Figs. 2 and 4, were tested. Fig. 9 gives the strain evaluation along four strain lines as the number of wet-dry cycles increased. As shown in Fig. 9, the strain of the 1st strain line was tensile, and the strain of the 4th strain line was compression. The concrete strains along the strain lines changed as the number of wet-dry cycles increased. Different strain values for same strain lines on different column specimens were observed due to the specified level of sustained load. The strains of Z5 gave the largest values for the tension line (1st strain line) and the lowest values for the compression line (4thstrain line) among the four columns Z2~Z5. The details of the variation of strains are shown in Fig. 9, where the strains for the 1st strain line were increased and the strains for the 4th strain line decreased as the level of the sustained load increased. There is no obvious difference in the strains between columns Z1 and Z2, where there were no cracks and no sustained load, when the environments were different.

3.1.3 Remaining Bearing Capacity of RC Column Specimens

At the age of 128d (28 days of concrete curing, 90 days of environment exposition, 10 days after load removal), RC columns and plain concrete specimens were tested. The concrete compressive strength and the ultimate loadwere analyzed here.

3.1.3.1 Compressive Strength of Plain Concrete

The compressive strengths of the concrete prisms were tested at the age of 128 days. The results are shown in Table 4. The compressive strengths were transformed to remaining percentages taking as a reference the strength inan atmospheric environment (or 0 cycles of wet-dry).

The compressive strength was tested at the age of 28 days with

Table 4. Compressive Strength of Plain Concrete Prisms

Prism Specimen	Compressive Strength (MPa)	Remaining Compressive
Specimen tested at 28 days	39.28	--
Wet-dry 0cycles	40.84	100%
Wet-dry 25 cycles	37.60	92%
Wet-dry 50 cycles	36.70	90%
Wet-dry 75 cycles	34.48	84%

one group of specimens. Then, at the age of 128 days, the remaining four groups of specimens were respectively tested after 0, 25, 50 or 75 wet-dry cycles of seawater. The compressive strength of the prism specimens decreased as the number of wet-dry cycles increased. Compared with the reference specimen (0 wet-dry cycles), the compression strength of the specimen with 75 wet-dry cycles decreased by 16%. Concrete strength usually increases with time during the first half year (Spiegel and Limbrunner (1998)).The reason why the compression strength of plain concrete decreased as the number of wet-dry cycles increased will be discussed in the section 3.2.2.

3.1.3.2 Remaining Mechanical Performance of RC Column Specimens

At the age of 128 days, the mechanical performances of RC column specimens Z1~Z5 were experimentally investigated by the eccentric compressive static loading test shown in Fig. 3, and the testing results are listed in Table 5. There are no obvious differences between the reference column Z1 (in the atmosphere) and column Z2 (in seawater wet-dry cycles). The remaining yield loads and ultimate loads of Z2-Z5 are shown in Fig. 10. As listed in Table 5 and shown in Fig. 10, the remaining yield load and ultimate load decreased as the maximum width of the initial crack increased. The ductility of the column specimens showed no clear tendency. The remaining yield load and ultimate load of column Z5 reduced to 91% of Z2, when the remaining mechanical performance was calculated with the function given in Eq. (1)

$$r_{zi}(\%) = (P_{zi}/P_{z2})100\% \quad (1)$$

Where P_{zi} is the remaining mechanical performance value of the specimen, andP_{z2} is the performance value of comparison column Z2.

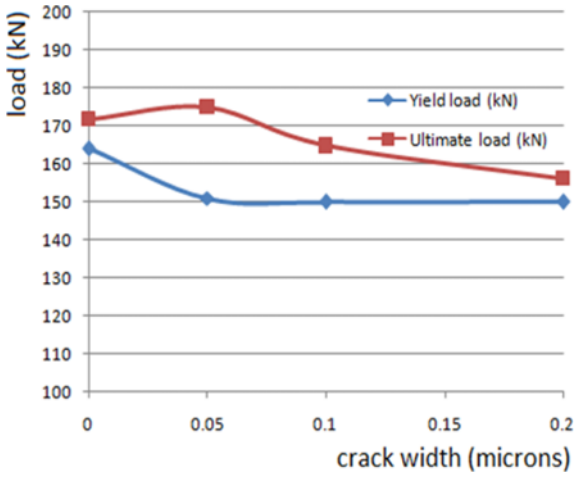

Fig. 10. Remaining Yield Load and Ultimate Load

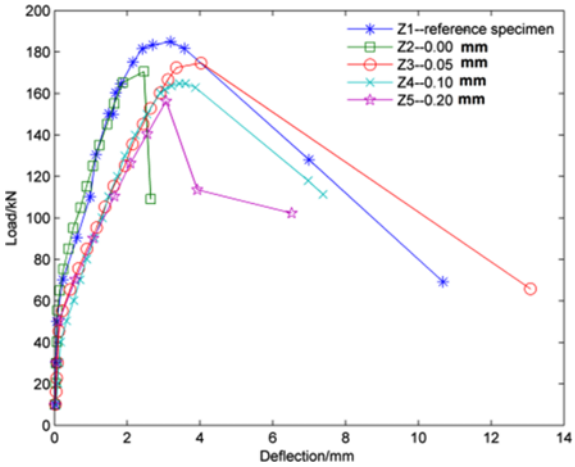

Fig. 11. Curves of Load Displacement at Mid-height

Comparison between the column without a crack (Z2) and the columns with cracks (Z3-Z5) gives a variation of the remaining yielding load percentage of approximately 8 to 9%. When the columns were loaded, the initial widths changed values from the initial 50, 100 and 200 microns, and the remaining yielding load percentage decreased from 92% to 91% between columns Z3

Table 5. Experimental Results and Their Variation

Designation	Yield of SteelBar		Ultimate Load		0.85 Pu of the Descent Stage		
Columns/ Crack Width	Load (kN)	Deflection (mm)	Load P_u (kN)	Deflection (mm)	Load (kN)	Deflection (mm)	Ductility
Z1/0	164.0	1.76	185.0	2.58	157.25	5.26	2.99
Z2/0	164.0	1.84	171.8	2.60	146.03	2.61	1.42
Remaining mechanical performance of column specimens Z2~Z5 compared with that of Z2							
Columns /crack width	Load	Deflection	Load Pu	Deflection	Load	Deflection	Ductility
Z2/0	100%	100%	100%	100%	100%	100%	100%
Z3/50 microns	92%	142%	102%	134%	102%	236%	166%
Z4/100 microns	91%	143%	96%	132%	96%	156%	109%
Z5/200 microns	91%	147%	91%	118%	91%	139%	95%

and Z4,before it gave the same value for column Z4 (100 microns) and Z5 (200 microns). Fig. 10 and Table 5 give the remaining yield load and ultimate load and the experimental results of their variations.

The curves of the eccentric compressive load and horizontal displacement at the mid-segment of the column were drawn in Fig. 11. As it is shown, the ultimate loads and stiffnesses of columns Z1~Z5 decreased as the width of the initial cracks increased, which means that the initial damage by sustained load is the main factor that contributed to structural performance decay.

3.1.4 Chloridecontent in the Concrete Tensile area of RC Column Specimens

After the static loading test, concrete cylinder samples of 50 mm diameter and 30 mm depth were drilled on surface C (tensile area) of the column specimens, and then each cylinder sample was subdivided along the depth into three slices. To study the crack effect, the surface C was divided into a central segment called CENTER and both wing areas called END, as shown in Fig. 12. It was clarified that all END segments were uncracked, the CENTER segments of columns Z3~Z5 were cracked and some CENTER segments of Z1~Z2 were uncracked. The slices were ground into fine powdery particles to test the free chloride content. The free chloride content in the samples was determined by Ion Selective Electrode Methods. The tested chloride contents

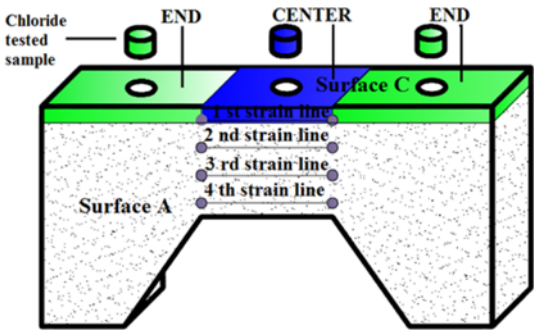

Fig. 12. Cylinder Samples to Test Chloride Content and Strain Lines of Columns

Table 6. Chloride Contents of Tensile Concrete

Column/Sample Location	Crack Situation	Depth 10 mm	Depth 20 mm	Depth 30 mm
Z1 /END	uncracked	0.0300	0.0172	0.0162
Z2 /END	uncracked	0.0800	0.0204	0.0196
Z3 /END	uncracked	0.1151	0.0230	0.0209
Z4/END	uncracked	0.1555	0.0381	0.0302
Z5 /END	uncracked	0.1794	0.0536	0.0372
Z1 /CENTER	uncracked	0.0307	0.0173	0.0176
Z2 /CENTER	uncracked	0.0834	0.0217	0.0215
Z3 /CENTER	cracked	0.1411	0.0255	0.0225
Z4/CENTER	cracked	0.1670	0.0404	0.0350
Z5 /CENTER	cracked	0.2011	0.0914	0.0603

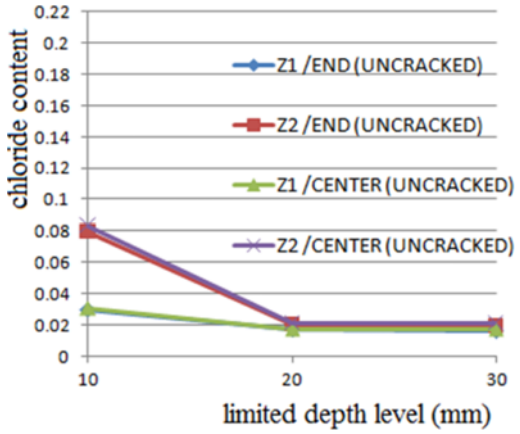

Fig. 13. Chloride Content on Unloaded Columns

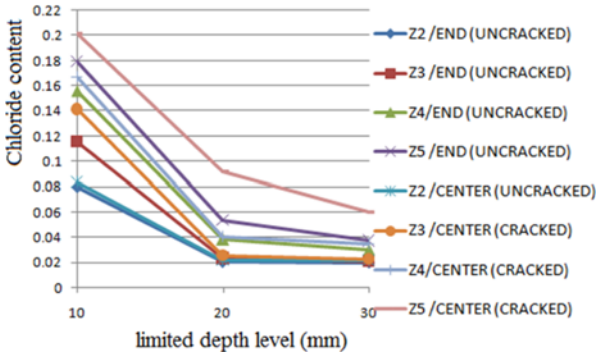

Fig. 14. Chloride Content in Seawater Cycled Column

are given in Table 6.

The chloride contents listed in the Table 6 are also plotted in Figs. 13 and 14 to highlight the effects of cracks on chloride penetration. The chloride content at different depths of columns Z1 (in atmosphere) and Z2 (in wet-dry cycles of seawater) are shown in Fig. 13. The chloride content was a little different at the depth of 0~10 mm, which means that the effect of the environment was weakened when the column had no load cracks, and the chloride content was nearly the same at the depth of 20~30 mm. The chloride content at different depths in the column specimens Z2~Z5 (in seawater wet-dry cycles) was shown in Fig. 14, and the chloride contents from adepth of 20 to 30 mm for columns Z2(without initial crack) and Z3(50 microns) are nearly the same for both areas of cracked and uncracked. The chloride contents of specimensZ3, Z4 and Z5 increased as the maximum width of the cracks increased, while the chloride contents in the cracked and uncracked areas of the column specimens were different. As shown in Fig. 14, the chloride content in the uncracked area of Z5 was larger than the chloride content in the cracked area of Z4 over the whole depth. The chloride content in the uncracked area of Z4 was larger than the chloride content in the cracked area of Z3, which indicates that the chloride content of the column specimen increased as the tensile strain (or sustained load level) increased, no matter if the concrete was cracked. As shown in Fig. 14, when the crack

width was larger than 100 microns, the differences in the chloride contents of the cracked area and the uncracked area became significantly larger.

3.2 Discussion

3.2.1 Effects of Crack Width on Chloride Content of RC Columns

As shown in Fig. 6 and Fig. 5(c) and in Table 3, the evolution of crack 3 on Z5 indicates that when the crack width is larger than 100 microns, the crack width tends to increase during the period of wet-dry cycles, mainly due to the coupled actions of the sustained load and wet-dry cycles of seawater. As shown in Fig. 5(b), when the crack width is 50 to 100 microns, the crack width tends to decrease during the period of wet-dry cycles. As shown in Fig. 5(a) and Fig. 7, crack 1 on Z3 (maximum 50 microns) vanished after 60 wet-dry cycles of seawater. That disappearance might be due to the self-healing capacity of concrete. The testing results for crack width indicated that the load-induced cracks with initial widths greater than 100 microns accelerated chloride penetration and hence expedited the corrosion initiation in the concrete structural members. In other words, once the crack width was greater than 100 microns, the concrete cover had little protective effect from reinforcement corrosion (ChunQing LI, 2001).

As shown in Fig. 14 and in Table 6, the chloride content of the tensile concrete increased as the crack width (or sustained load level) increased. When the initial crack width was not larger than 100microns (here for column specimens Z2, Z3 and Z4), the differences in chloride contents for the column specimens were small in both the cracked and uncracked areas of concrete. When the initial crack width was larger than 100 microns (here for column specimen Z5), the chloride content of the cracked concrete is obviously different from the chloride content of the uncracked (tensile) concrete. Longitudinal tensile strains on corroded beams under a constant sustained load are influenced by the magnitude of the applied load but mostly by the level of corrosion of the steel bars (Malumbela *et al*., 2009).When the crack widths become larger than 100 microns, it is possible for ions and oxygen to reach the reinforcement after the carbonation of the concrete and create rust (Audenaert *et al*., 2009; Ismail *et al*., 2004). The 100 micron crack width might be a limit for the RC structural member under normal working conditions.

3.2.2 Reduction of Concrete Strength

As listed in Table 4, after the action of the wet-dry cycles of seawater, the compressive strength of the concrete prisms decreased rapidly. The literature review showed that in a marine environment, carbon dioxide is subject to carbonation and reacts with aluminates and calcium silicate hydrates, i.e., the major constituents of hydrated cement (Basheer *et al.*, 2007). Furthermore, under the influence of carbon dioxide (CO_2) from the air, the carbonation process occurs. The free lime in the concrete cement paste is bound, and the alkalinity is lost.The pH values of the concrete drop from 12.5~13 to 8.5~9 (Schueremans *et al*., 2007). Pommer Sheim and Clifton (1985) demonstrated that in sea water, degradation mechanisms can be due to the reaction that involves the replacement of $ca(oh)_2$ in concrete by gypsum ($caso_4.2h_20$) and an expansive process that involves the reaction of sulfate ions with calcium aluminates hydrate to give ettringite (3cao. a1203. 3caso4.31 h20). The experimental condition mentioned in this subpart is non-cracked or non-sustained load. Thus, the compressive strength of concrete decreasing as the number of wet-dry seawater cycles increases can be explained by multiple chemical reactions that might occur between concrete and seawater.

4. Conclusions

The coastal chloride environment and normal working conditions of Reinforced Concrete (RC) structures were simulated in the laboratory. Different widths of the initial crack at 50 microns, 100 microns, and 200 microns were induced in RC column specimens by different levels of eccentric compressive load. After 90 wet-dry cycles of sea water and atmosphere actions, the remaining mechanical performance and chloride content of RC columns were tested. The following conclusions were drawn.

1. During all of the experimental processes including seawater wet-dry cycles, when the maximum width of the initial crack was less than 50 microns, the crack tended to vanish due to the self-healing capacity of concrete. In addition, when the maximum width of the crack was not larger than 100 microns, the crack tended to decrease slightly and remained relatively constant. The width of the crack tended to increase when the maximum width of the initial crack was larger than100 microns.
2. After 90 wet-dry cycles of seawater, both the yielding load and the ultimate load of the RC column specimens decreased as the width of the initial crack (or the level of the sustained load) increased. However, deflection caused by both the yielding load and ultimate load showed no clear tendency.
3. Both tensile strain and crack opening width were parameters that contributed to the chloride penetration in the tensile area of the RC structures. The chloride content of the tensile concrete increased as the tensile strain (or sustained load) increased, no matter if the concrete was cracked, and when the crack width was larger than 100 microns, the difference in chloride content between the cracked area and the uncracked area becameobviously larger

Acknowledgements

This work is a part of projects financially supported by the National Natural Science Fund of China (NSFC) Grant No. 51578031 and the Fund of the State Key Laboratory of Subtropical Building Science (FSKLSBS) South China University of Technology Grant No. 2016ZA03. The authors gratefully acknowledge the funding from the NSFC and FSKLSBS.

References

Audenaert, K., Marsavin, L., and De Schutter, G. (2009). "Influence of cracks on the service life of concrete structures in a marine environment." *Key Engineering Materials.,* Vol. 399, (2009), pp. 153-160.

Basheer, L., Kroop, J., and Cleland, D. J. (2001). "Assessment of the durability of concrete from its permeation properties: A review" *Construction and Building Materials*, Vol. 15, Nos. 2-3, pp. 93-103.

Capozucca, R. and Cerri, M. N. (2000). "Identification of damage in reinforced concrete beams subjected to corrosion." *ACI Structural Journal*, N.97-S92, pp. 902-909.

Djerbi, A., Bonnet, S., Khelidj, A., and Baroghel-bouni, V. (2008). "Influence of traversing crack on chloride diffusion into concrete." *Cement and Concrete Research,* Vol. 38, No. 6, pp. 877-883, DOI: 1016/j.cemconres.2007.10.007.

Gowripalan, N., Sirivivatnanon, V., and Lim, C. C. (2000). "Chloride diffusivity of concrete cracked in flexure." *Cement and Concrete Research*, Vol. 30, No. 5, pp. 725-730.

Gu, C., YE, G., and SUN, W. (2015). "A review of the chloride transport properties of cracked concrete: Experiments and simulations", *Journal of Zhejiang University-SCIENCE A (Applied Physics & Engineering),* Vol. 16, No. 2, pp. 81-92 ISSN 1673-565x(print); ISSN 1862-1775(online).

Ismail, M., Toumi, A., François, R., and Gagné, R. (2004). "Effect of crack opening on the local diffusion of chloride in inert materials." *Pergamon Cement and Concrete Research*, Vol. 34, No. 4, pp. 711-716, DOI: 10.1016/j.cemconres.2003.10.025.

Ismail, M., Toumi, A., François, R., and Gagné, R. (2008). "Effect of crack opening on the local diffusion of chloride in cracked mortar samples." *Cement and Concrete Research,* Vol. 38, Nos. 8-9, pp. 1106-1111.

Jia, C., Li, Y., and Ren, Q. (2010). "Cracking analysis of high concrete gravity dams under floodwater and seismic effects." *IEEE National Program on Key Basic Researcj (973 program)* (2007CB714104), 798-1-4244-4813-5/10/:

Khan, I., Francois, R., and Castel, A. (2014). "Prediction of reinforcement corrosion using corrosion induced cracks width in corroded reinforced concrete beams." *ELSEVIER Cement and Concrete Research*, Vol. 56, (2014), pp. 84-96, DOI: 10.1016.

Khan M. Iqbal (2012). "Comparison of chloride ion penetration and diffusion of high-performance concrete." *KSCE Journal of Civil Engineering,* Vol. 16, No. 5, pp. 779-784, DOI: 10.1007/s12205-012-1237-x.

Li, C. Q. (2001). "Initiation of chloride-induced reinforcement corrosion in concrete structural members-experimentation." *ACI Structural Journal*, No. 98-S48, pp. 502-510.

Lu, C., Jun, W., and Liu, R. (2011). "Probabilistic lifetime assessment of marine reinforced concrete with steel corrosion and cover cracking." *Chinese Ocean Engineering Society and Springer-Verlag Berlin Heidelberg*, Vol. 25, No. 2, pp. 305-318, DOI: 20.2007/s133344-011-0025-6, ISSN 0809-5487.

Malumbela, G., Moyo, P., and Alexander, M. (2009). "Behaviour of RC beams corroded under sustained service loads." *ELSEVIER Construction and Building Materials,* Vol. 23, No. 11, pp. 3346-3351, DOI: 10.1016/j.conbuildmat.2009.06.005.

Marsavin, L., Audenaert, K., De Schutter, G., Faur, G., and Marsavina, D., (2009) "Experimental and numerical determination of the chloride penetration in cracked concrete." *ELSEVIER Construction and Building Materials*, Vol. 23, No. 1, pp. 264-274.

Noël, M. and Soudki, K. (2014). "Estimation of the crack width and deformation of FRP-reinforced concrete flexural members with and without transverse shear reinforcement." *Elsevier Engineering Structures*, Vol. 59, pp. 393-398.

Pacheco, J., Šavija, B., Schlangen, E., and Polder, R. B. (2014). "Assessment of cracks in reinforced concrete by means of electrical resistance and image analysis." *ELSEVIER Construction and Building Materials,* Vol. 65, (2014), pp. 417-426.

Pommersheim, J. and Clifton, J. (1985). "Prediction of concrete service-life." *Materials and Structures,* Vol. 18, No. 1, pp. 21-30.

Schueremans Luc, Van Gemert Dionys, and Giessler Sabine (2007). "Chloride penetration in RC-structures in marine environment – Long term assessment of a preventive hydrophobic treatment." *ELSEVIER Construction and Building Materials,* Vol. 21 (2007), 1238-1249.

Spiegel, L. and Limbrunner, G. F. (1998). "Reinforced Concrete Design." book. fourth edition.

Yoon, I.-S. and Schlangen, Erik (2014). "Comparison of chloride ion penetration and diffusion of high-performance concrete." *KSCE Journal of Civil*, Vol. 18, No. 1, pp. 188-198, DOI: 10.1007/s12205-014-0196-9.

Zhao, Y., Yu, J., and Jin, W. (2011). "Damage analysis and cracking model of reinforced concrete structures with rebar corrosion." *ELSEVIER Corrosion Science*, Vol. 53, No. 10, pp. 3388-3397, DOI: 10.1016/j.corsci.2011.06.018.